

Compliant Topology Optimization for Planar Passive Flap Micro Valve

Gil Ho Yoon

School of Mechanical Engineering, Hanyang University, 133-791, Korea

This paper reports the compliant topology optimization for planar passive flap micro valve considering fluid-structure interaction with a monolithic approach. Although flap valve type check valve is easy to manufacture and use for the applications for Bio/Nano/MEMS, its structural optimization has been seldom conducted so far. The size of the Bio/Nano/MEMS devices becomes smaller and the simple straight type micro valve structure is required to be optimized considering fluid speed. To address this optimization problem, the structural topology optimization scheme which designs optimal topologies is applied for a flap type check valve structure. To consider the coupling effects of fluid domain and structural domain, the monolithic finite element approach is employed. In the new analysis approach, solid domain is simulated by introducing the inverse permeability in the Navier-Stokes equation and the fluid stress filter in the linear elasticity equation. Also it is a new idea that fluid domain is simulated by finite elements with a weak Young's modulus in the linear elasticity equation. The mutual couplings between fluid and structure are considered by the introduction of the deformation tensor which is one of the basic concepts of the continuum mechanism. By distributing material properties inside a design domain for compliant flap, optimal flap structures can be constructed with different fluid speeds. By investigating the optimal layouts of several passive flap designs, we prove that the structural topology optimization can provide optimal layouts for Bio, Nano, and MEMS applications.

Keywords: Passive Flap Structure, Topology Optimization, Fluid-Structure Interaction.

1. INTRODUCTION

1.1. Topological Optimization for μ -TAS

In the field of bio, chemical and nano analysis, it is necessary to develop small and portable but cheap systems for sensors and actuators.^{1–6} With the help of the development of micro mechanical fabrication techniques for the last few decades, many small and integrated components and μ -TAS systems have been proposed and fabricated.^{1–6} Components and systems being miniaturized, one of the benefits from them is the fast, chemical, electrical, mechanical and fluid dynamical responses. Partially due to their miniaturizations, their performances are highly dependent on more than one physics system and it is necessary to consider multiphysics systems to predict the stationary as well as dynamic responses of the micro fluid handling components and systems such as valves, pumps and sensors.^{1–6} Thus many computational theories have been proposed to effectively analyze these multiphysics systems and many structural optimization methods also have been proposed and applied.^{4, 7–15}

In this research, we aim to optimize a compliant passive check valve by applying one of the structural optimization methods, topology optimization, considering the fluid and structure interaction. Because topology optimization allows us to change connectivities inside design domain as shown in Figure 1(a), the conventional computational analysis method for fluid and structure interaction cannot be incorporated. Therefore our previous contribution for fluid-structure interaction was employed here to topologically optimize the flap type check valve in Figure 1(b).^{8, 16–19}

1.2. Passive Check Valve

In fluid handling nano and micro systems, small check valves play an important role.^{1–6} Recently some innovative approaches to actively direct fluid streams have been proposed using piezoelectricity, electricity and etc. and this kind of check valve provides the possibility to build complex μ -TAS systems. On the other hands, a direction dependent pressure drop over the valve also

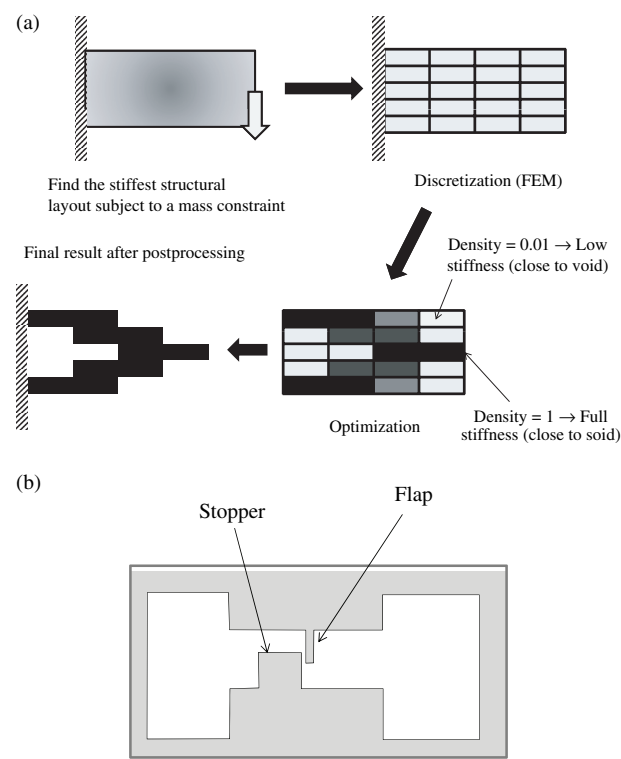


Figure 1. (a) Topology optimization practice for structural problem⁹ and (b) micro flap type check valve.⁶

can be obtained with the differences in flow resistivity due to the geometry differences, i.e., the diffuser-nozzle principle or the reduction of the cross-area for reversed fluid. In addition to these, the flap type valve is also proposed. Unlike the other check valves, this kind of check valve has some elastic and rigid parts and the movements of the

elastic parts due to fluid pressure make spatial fluid gaps closed.^{4,5} Normally, the flap valve consists of a compliant plate, clamped at one side as shown in Figure 1(b). If flow is applied at the left, the plate will bend, i.e., open, and the fluid flows through. In the opposite direction, the plate will be pushed against the structure which closes the fluid gap.

For the modeling the pressure drop over the valve and the movement as a function of the flow-rate, we have to deal with the mutual coupling between solid mechanical and fluid mechanical domain. The pressure drop over the valve can be computed from the flow profile of the fluid and the flow-profile is related to the pressure-induced geometrical deformation of the valve; fluid-structure interaction. The multiphysics problem can be solved in two ways: staggered analysis, and monolithic analysis as shown in Figure 2.^{1, 16, 17, 20–24} But these existing approaches cannot be easily incorporated with the topology optimization allowing the topological changes and our previous contribution shown in Figure 3 is employed for the topology optimization for the check type valve design in Figure 1(b).

The rest of this paper is organized as follows. First, we present monolithic fluid and structure interaction analysis. Here the coupled fluid equation and the coupled linear elasticity equation are presented and the main differences compared with the conventional computational approaches are discussed. Then the topology optimization formulations are developed to design the check type valve in Figure 1(b) and we present the optimized designs with two different flows. Here we discuss the differences compared with the conventional bar type check valve. Finally, the conclusions and observations of this research are given in the conclusions section.

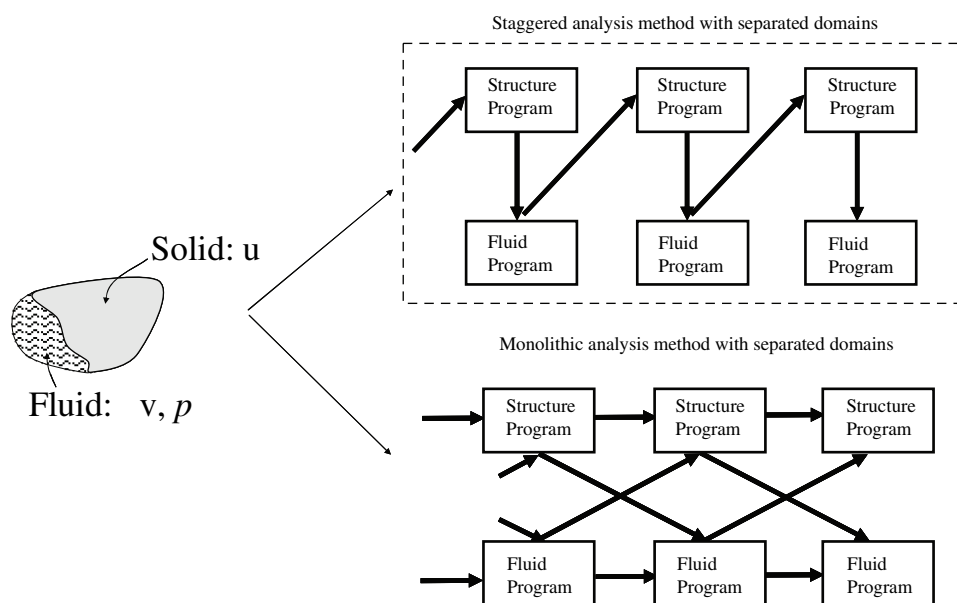


Figure 2. Staggered and monolithic approach for fluid and structure interaction.

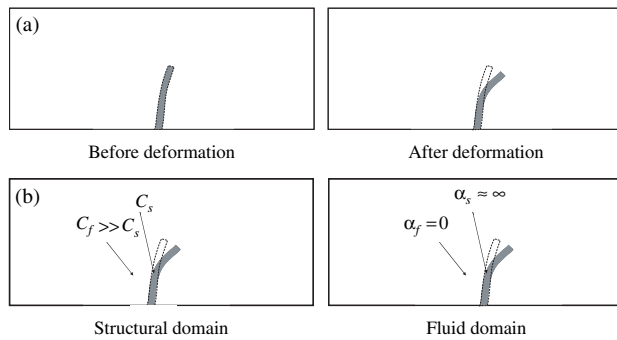


Figure 3. The concepts of the present monolithic analysis method for steady-state fluid-structure interaction problem without explicit interaction boundaries: (a) deformed and undeformed states and (b) material values for structural and fluid domains (C_s and C_f are Young's moduli of the structure and fluid and α_s and α_f are the inverse coefficients of the permeability of the solid and fluid, respectively).

2. MONOLITHIC APPROACH FOR FLUID-STRUCTURE INTERACTION

The fluid and structural domains change their configurations continuously during a topology optimization iterative procedure^{16, 17} that is almost impossible to be implemented in the existing staggered or monolithic approaches. Therefore, in our previous contributions, the concept of the deformation tensor (or the deformation gradient) was introduced. In continuum mechanics theory, the finite deformation tensor, \mathbf{F} , is defined as the partial differential of the current coordinate, \mathbf{x} , with respect to the undeformed coordinate, \mathbf{X} ,

$$\mathbf{x} = \mathbf{X} + \mathbf{u} \quad (1)$$

where the structural displacements map between \mathbf{x} and \mathbf{X} . In our previous contributions, this deformation tensor \mathbf{F} was used to correlate the differential operators and integral operators of the two configurations as well as the quantities of the two configurations such as mass density, strain, and volume^{16, 17}

$$\mathbf{F} = \frac{\partial \mathbf{x}}{\partial \mathbf{X}}, \quad \nabla_{\mathbf{X}} = \mathbf{F}^T \nabla_{\mathbf{x}}, \quad \nabla_{\mathbf{x}} = \mathbf{F}^{-T} \nabla_{\mathbf{X}} \quad (2)$$

$$\int_{\Omega} (\cdot) d\Omega = \int_{\Omega} (\cdot) \|\mathbf{F}\| d\Omega \quad (3)$$

$${}^0\Omega = {}^0_{ms}\Omega \cup {}^0_{mf}\Omega, \quad {}^t\Omega = {}^t_{ms}\Omega \cup {}^t_{mf}\Omega \quad (4)$$

Here the spatial differentiations at the deformed domain and the undeformed domain are denoted by $\nabla_{\mathbf{x}}$ and $\nabla_{\mathbf{X}}$, respectively. Here the undeformed fluid and solid domain are denoted by ${}^0_{mf}\Omega$ and ${}^0_{ms}\Omega$. The deformed fluid and solid domain are denoted by ${}^t_{mf}\Omega$ and ${}^t_{ms}\Omega$, respectively. With these deformation tensors, the Navier-Stokes equations after the structural deformation, \mathbf{u} , can be transformed into one defined at the undeformed domain.

$$\begin{aligned} & - \int_{\Omega} \delta \mathbf{v}^T \{ \rho (\mathbf{v} \cdot \mathbf{F}^{-T} \nabla_{\mathbf{X}} \mathbf{v}) \} \|\mathbf{F}\| d\Omega \\ & = \int_{\Omega} \mathbf{F}^{-T} \nabla_{\mathbf{X}} \delta \mathbf{v}^T \mathbf{T}_f \|\mathbf{F}\| d\Omega + \int_{\Omega} \alpha \delta \mathbf{v}^T \mathbf{v} \|\mathbf{F}\| d\Omega \\ & - \int_{\Gamma_{p^*}} p_{p^*} \mathbf{n} d\Gamma \end{aligned} \quad (5)$$

$$- \int_{\Omega} \delta p^T \{ (\nabla_{\mathbf{x}} \cdot \mathbf{v}) \} \|\mathbf{F}\| d\Omega = 0 \quad (6)$$

$$\mathbf{T}_f = -p\mathbf{I} + \mu(\nabla_{\mathbf{x}} \mathbf{v} + \nabla_{\mathbf{x}} \mathbf{v}^T) \quad (7)$$

where the fluid velocity field and pressure of an incompressible flow are described by \mathbf{v} and p , respectively. The fluid density and the dynamic viscosity for Newtonian flow are denoted by ρ and μ , respectively. The Neumann boundary condition for the applied pressure is defined at Γ_{p^*} with the normal vector, \mathbf{n} . The inverse coefficient of permeability of the fluid is α . With a sufficiently large value of α , the velocities along the interfacing boundaries become zero that is one of the main concepts in topology optimization for fluid domain. Thus, a very large value can be assigned to the solid domain for zero velocities inside the structural domain and at the interface boundaries as follows:

$$\begin{cases} \alpha = \alpha_{\max} \gg 0 & \text{for solid or interface boundaries} \\ \alpha = 0 & \text{for fluid} \end{cases} \quad (8)$$

As same with the Navier-Stokes equation, the linear elasticity domain of the deformed domain is transformed into one of the undeformed domain with the deformation tensor. Note that the external energy due to the fluid stress at the interaction boundary is dependent on the structural displacement, the deformation tensor is used after applying the divergence theory for the right side of the Eq. (9).^{16, 17}

$$\begin{aligned} \int_{\Omega} \delta \mathbf{S}^T \cdot \mathbf{T}_s d\Omega & = \int_{\Omega} \Psi \cdot \mathbf{F}^{-T} \delta \mathbf{S}(\mathbf{u}, \delta \mathbf{u})^T \cdot p \|\mathbf{F}\| d\Omega \\ & + \int_{\Omega} \Psi \cdot \mathbf{F}^{-T} \delta \mathbf{u} \cdot \nabla_{\mathbf{X}} p \|\mathbf{F}\| d\Omega \end{aligned} \quad (9)$$

$$\Psi = \begin{cases} 1 & \text{for solid domain} \\ 0 & \text{for fluid domain} \end{cases} \quad (10)$$

$$\mathbf{S} = \frac{1}{2}(\nabla_{\mathbf{x}}^T \mathbf{u} + \nabla_{\mathbf{x}} \mathbf{u}), \quad \mathbf{T}_s = \mathbf{C} \mathbf{S} \quad (11)$$

$$\mathbf{S}(\mathbf{u}, \delta \mathbf{u}) = \frac{1}{2}(\nabla_{\mathbf{x}}^T \mathbf{u} + \nabla_{\mathbf{x}} \mathbf{u}), \quad \nabla_{\mathbf{x}} = \mathbf{F}^{-T} \nabla_{\mathbf{X}} \quad (12)$$

where the linear strain \mathbf{S} and the associate stress \mathbf{T}_s are defined as above. The linear constitutive matrix is denoted by \mathbf{C} . By solving the coupled Eqs. (5) and (6) for fluid and (9) for solid, the steady state fluid-structure interaction system can be analyzed successfully.

For the illustrative analysis numerical example, we consider the structure shown in Figure 4. The two sides are clamped and there is pressure at the upper side. We can compare the displacements and stress solutions with the standard FE model of Figure 4(a). The boundary conditions used for the present scheme are depicted in Figure 4(b). As shown in Figure 5, the structural displacements of the structural finite element and present methods agree well with each other.

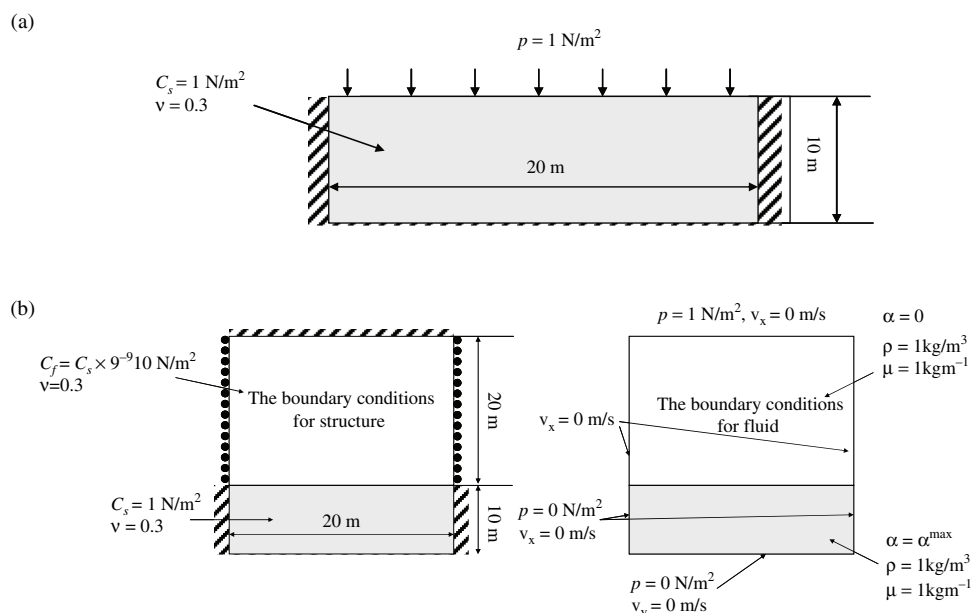


Figure 4. Rectangular box with clamped sides (plane stress, 80×40 quad elements): (a) pure structural model and (b) model used for present monolithic approach.

3. TOPOLOGY OPTIMIZATION DESIGN FOR CHECK FLAP VALVE

To design a compliant flip check valve, the design domain and the boundary condition in Figure 6 are considered. The analysis domain is $2200 \mu\text{m}$ by $1300 \mu\text{m}$ and the design domain is set to design not only the check valve but also the stopper shape. It means if necessary the optimization algorithm can put some material for stopper channel. For an optimization formulation, the following formulation is considered.

$$\begin{aligned} & \text{Max } U_{\text{Open}} - U_{\text{Close}} \\ & \text{Subject to } V \leq V^* \end{aligned} \quad (13)$$

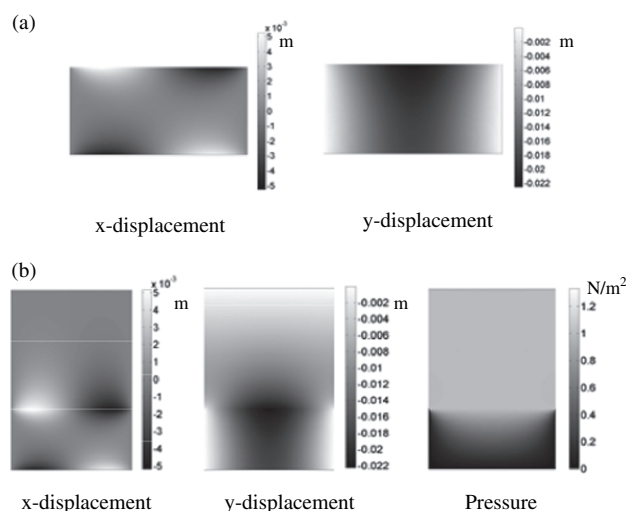


Figure 5. Analysis results: (a) displacements of pure structural model (Fig. 4(a)) and (b) displacements and pressure of present model (Fig. 4(b)).

where the structural displacement due to the flow from the right side to the left side is denoted by U_{Open} and the structural displacement due to the flow from the left side to the right side is denoted by U_{Close} . The purpose of the objective is that when the fluid flows toward the right side, the structure should open and the tip displacement in the x -direction should be maximized whereas for the fluid flowing toward the left side the structure will close and the tip displacement in the x -direction should be minimized. The volume and the maximum volume are denoted by V and V^* , respectively. The reason to consider the mass constraint is to make the optimization problem stable although the mass constraint is not important in Nano or MEMS structure. The Method of Moving Asymptotes is used for an optimizer.²⁵ The overall design process is depicted in Figure 8.

As stated and illustrated in Figures 4 and 5, for a successful complex FSI analysis, the proper material properties of fluid and elastic structure should be assigned. For a successful structural topology optimization for FSI structure, a proper material interpolation scheme to relax the difficult 0–1 topology problem should be devised as (14) to (16). In this research, the following material interpolation schemes based on the Solid Isotropic Material with Penalization (SIMP) are employed for the interpolations of the two physics. The intermediate densities are used as a means for a gradient-based method for topology optimization.

$$\text{Young's modulus: } C(\gamma) = (C_S - C_F)\gamma^n + C_F \quad (14)$$

$$\text{Fluid stress filter: } \Psi(\gamma) = \gamma^n \quad (15)$$

$$\text{Inverse permeability: } \alpha(\gamma) = \alpha_{\max} \gamma^{n_f} \quad (16)$$

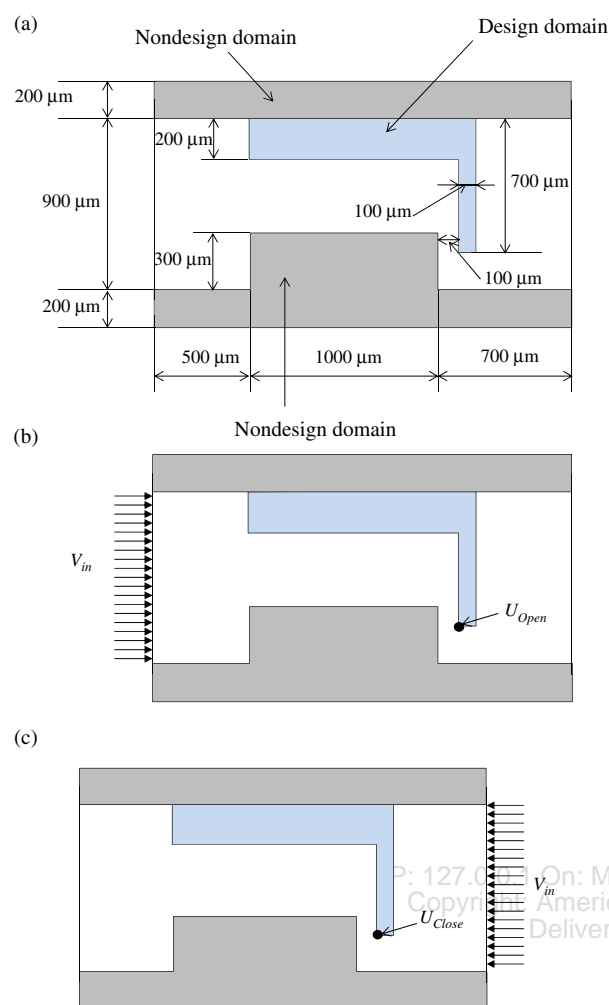


Figure 6. The design domain and the boundary condition. ($C_s = 1$ MPa, $C_F = C_s \times 10^{-3}$, $\nu = 0.3$, $\alpha_{max} = 10^9$, $n = 3$, $n_f = 5$, $\rho = 1000$ Kg/m³, $\mu = 1.002 \times 10^{-3}$ Kg · m⁻¹).

where the density design variable is denoted by γ as shown in Figure 7 and the penalization factors are denoted by n and n_f . Note that it is possible to use different penalization factors for the above interpolation functions and some different local optimal structures are obtained.

By running the optimization process of Figure 8, the designs of Figure 9 can be obtained with the different flow inputs. With a lower velocity, i.e., $V_{in} = 0.01$ m/s, the curved beam type can be obtained. By observing the flow lines and the deformation in Figure 10, it turns out that

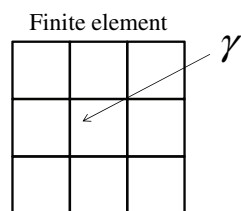


Figure 7. The design variable in the Solid Isotropic Material with Penalization (SIMP).

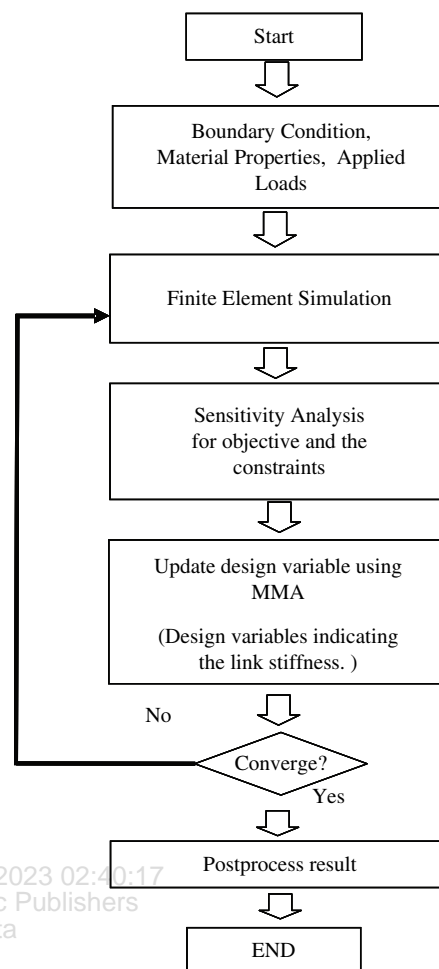


Figure 8. The developed optimization procedure.

the design opens and closes depending on the direction of fluid flow and there are some curved structures near to the upper wall to maximize the compliance, that is the inverse the structure. Then the same optimization process

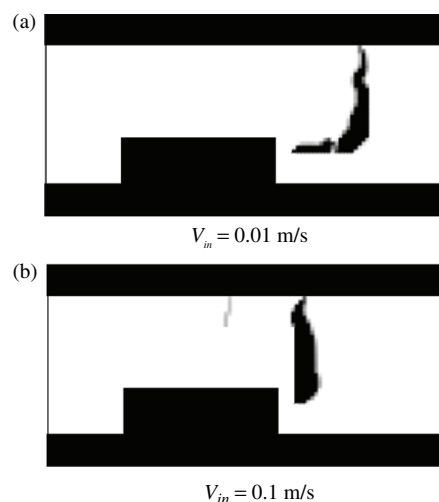


Figure 9. The designs with different velocities.

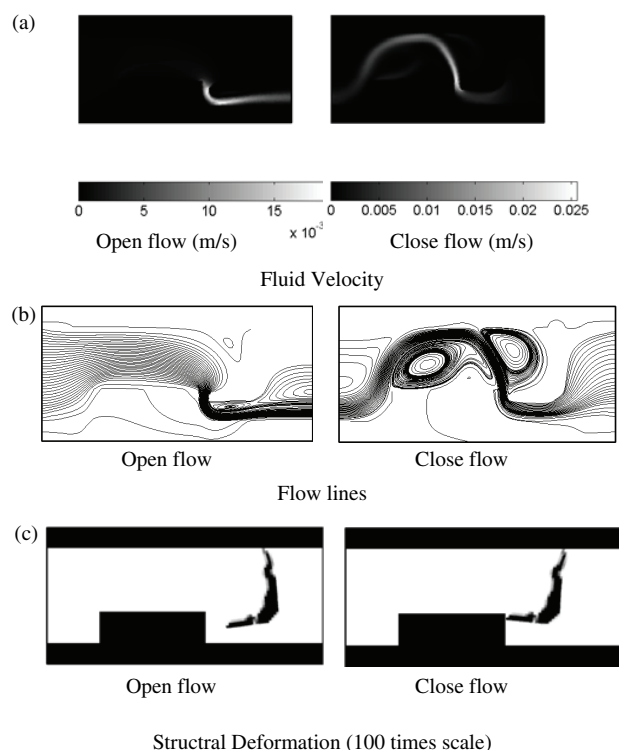


Figure 10. Fluid velocity, flow lines and structural deformation of the design Figure 9(a) with $V_{in} = 0.01$ m/s ($U_{Open} = 9.19 \mu\text{m}$, $U_{Close} = -10.16 \mu\text{m}$).

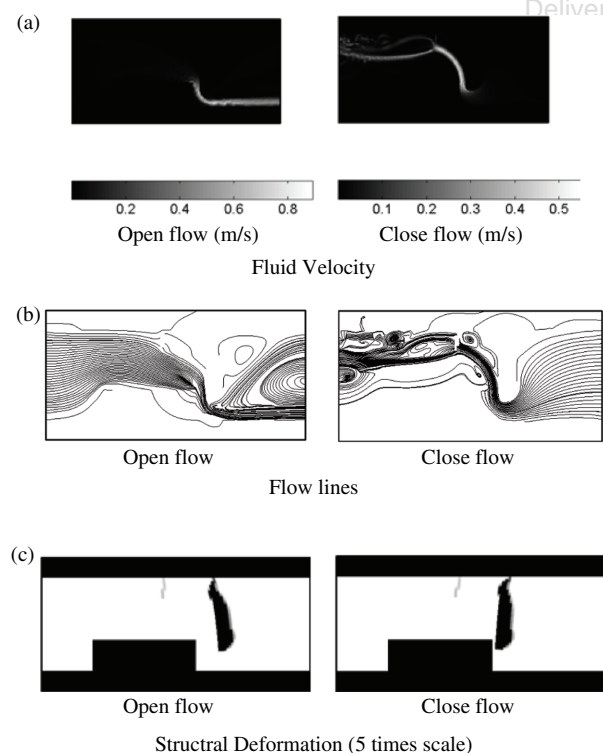


Figure 11. Fluid velocity, flow lines and structural deformation of the design Figure 9(b) with $V_{in} = 0.1$ m/s ($U_{Open} = 228.09 \mu\text{m}$, $U_{Close} = -159.77 \mu\text{m}$).

with $V_{in} = 0.1$ m/s provides the design of Figure 9(b). Here it can be postulated that the straight bar appear and similar to the design of Figure 9(a), the curved structure appears near to the upper wall again. With this high velocity speed input, the fluid force exerted on the structure is also increased and the displacements are also increased as expected as shown in Figure 11.

4. CONCLUSION

In this research, the topological optimization for a compliant planar passive flap micro valve is conducted in the framework of the monolithic fluid-structure interaction analysis. As the topology optimization can provide an optimal topology with a given initial configuration, it can be used for many applications for the design of Bio, Nano, and Micro system. However for its applications toward fluid structure interaction system, it becomes complicated as not only the material properties but also the governing equations should be altered that is difficult from a structural optimization point of view. Therefore a new monolithic analysis method coupling the two governing equations with the structural deformation tensor is employed. By interpolating the material properties, it is possible to conduct compliant topology optimization for planar passive flap micro valve. With the present approaches, the effect of the fluid velocity is observed and the optimal designs rather than a straight flap can be obtained. For a future research topic, the designs should be manufactured to verify their effectiveness.

Acknowledgment: This work was supported by the National Research Foundation of Korea (NRF) grant funded by the Korea government (MSIP) (No. 2013R1A2A1A01015171).

References and Notes

1. V. Ostasevicius, R. Dauksevicius, R. Gaidys, and A. Palevicius, *J. Sound Vib.* 308, 660 (2007).
2. I. Izzo, D. Accoto, A. Menciassi, L. Schmitt, and P. Dario, *Sensor Actuat. A-Phys.* 133, 128 (2007).
3. X. F. Leng, J. H. Zhang, Y. Jiang, J. Y. Zhang, X. C. Sun, and X. G. Lin, *Sensor Actuat. A-Phys.* 195, 1 (2013).
4. H. Andersson, W. van der Wijngaart, P. Nilsson, P. Enoksson, and G. Stemme, *Sensor Actuat. B-Chem.* 72, 259 (2001).
5. H. Jerman, *J. Micromech. Microeng.* 4, 210 (1994).
6. R. E. Oosterbroek, S. Schlautmann, J. W. Berenschot, T. S. J. Lammerink, A. van den Berg, and M. C. Elwenspoek, Modeling and validation of flow-structure interactions in passive micro valves, *IAMMM Int. Conf. Modeling and Simulation of Microsystems*, Santa Clara, CA, USA (1998), p. 528.
7. W. Akl, *International Journal for Computational Methods in Engineering Science and Mechanics* 11, 337 (2010).
8. C. Andreasen and O. Sigmund, *Struct. Multidiscip. O* 43, 693 (2011).
9. M. P. Bendsøe and O. Sigmund, *Topology Optimization: Theory, Methods, and Applications*, Springer, Berlin, New York (2003), p. xiv.
10. F. J. Blom, *Comput. Method Appl. M* 167, 369 (1998).

11. T. Borrvall and J. Petersson, *Int. J. Numer. Meth. Fl* 41, 77 (2003).
12. V. J. Challis and J. K. Guest, *Int. J. Numer. Meth. Eng.* 79, 1284 (2009).
13. A. Gersborg-Hansen, O. Sigmund, and R. B. Haber, *Struct. Multidiscip O* 30, 181 (2005).
14. S. Kreissl, G. Pingen, A. Evgrafov, and K. Maute, *Struct. Multidiscip O* 42, 495 (2010).
15. J. Y. Noh and G. H. Yoon, *Adv. Eng. Softw.* 53, 45 (2012).
16. G. H. Yoon, *Int. J. Numer. Meth. Eng.* 82, 591 (2010).
17. G. H. Yoon, *Comput. Method Appl. M* 209, 28 (2012).
18. G. H. Yoon, J. S. Jensen, and O. Sigmund, *Int. J. Numer. Meth. Eng.* 70, 1049 (2007).
19. G. H. Yoon and O. Sigmund, *Comput. Method Appl. M* 197, 4062 (2008).
20. R. van Loon, P. D. Anderson, F. N. van De Vosse, and S. J. Sherwin, *Comput. Struct.* 85, 833 (2007).
21. J. Vierendeels, K. Dumont, and P. R. Verdonck, *J. Comput. Appl. Math.* 215, 602 (2008).
22. Q. L. Liu and O. V. Vasilyev, *J. Comput. Phys.* 227, 946 (2007).
23. A. Legay, J. Chessa, and T. Belytschko, *Comput. Method Appl. M* 195, 2070 (2006).
24. K. C. Park, C. A. Felippa, and R. Ohayon, *Comput. Method Appl. M* 190, 2989 (2001).
25. K. Svanberg, *Int. J. Numer. Meth. Eng.* 24, 359 (1987).

Received: 23 September 2013. Accepted: 20 October 2013.

IP: 127.0.0.1 On: Mon, 20 Nov 2023 02:40:17
Copyright: American Scientific Publishers
Delivered by Ingenta